RNase III is required for localization to the nucleoid of the 5′ pre-rRNA leader and for optimal induction of rRNA synthesis in *E. coli*

FRANCISCO MALAGON[1]
Laboratory of Molecular Biology, National Cancer Institute, National Institutes of Health, Bethesda, Maryland 20892-4264, USA

ABSTRACT

It has recently been demonstrated that ribosomes are preferentially localized outside the nucleoid in *Escherichia coli*, but little is known about the spatial regulation of pre-rRNA processing. In this work, I investigate the cellular distribution of leader pre-rRNAs using RNA-FISH. In contrast to mature rRNA, the 5′ proximal leader region associates with the nucleoid, and this association occurs in an RNase III-dependent manner. Moreover, RNase III plays a role in the rapid induction of ribosomal operons during outgrowth and is essential in the absence of the transcriptional regulator Fis, suggesting a linkage of transcription and RNA processing for ribosomal operons in *E. coli*.

Keywords: Pre-rRNA; RNase III; nucleoid; ribosomal operon; Fis

INTRODUCTION

The coupling of processes required for gene expression is widely recognized to have an important regulatory role (Maniatis and Reed 2002). This coupling ensures a quantitative and qualitative control on the final outcome of the transcription process (Maniatis and Reed 2002; Muhlemann and Jensen 2012). One of the first examples of coupling discovered was the cotranscriptional translation of mRNAs in bacteria (Miller et al. 1970). This phenomenon is thought to have a role in mRNA quality control by averting unproductive transcription events. In eukaryotes, where the two processes occur in different cellular compartments, the principal quality control mechanisms are established at different levels, i.e., messenger ribonucleoprotein (mRNP) nuclear export control and nonsense-mediate decay RNA degradation, while roughly keeping a similar objective (Luna et al. 2008; Dahan and Choder 2013). Although translation-dependent mRNA stabilization (protection from RNA degradation of productive transcripts) provides a straightforward quality control mechanism for mRNAs, faithful noncoding RNA production has to be monitored by alternative means, such as detection of proper association of RNP proteins or correct RNA folding.

Ribosomes are the most abundant RNPs in the cell and are roughly composed of two-thirds rRNA (ribosomal RNA) and one-third ribosomal proteins. Transcription of rRNA operons is strictly modulated to fine-tune their synthesis with the cellular needs for protein production. The common view is that this regulation has a major energetic cost component. That is, the cells should adjust rRNA synthesis to satisfy the demand for ribosome production while avoiding excess rRNA (Schneider et al. 2002). Likewise, environmental alterations that lead to a lower requirement for protein synthesis promote the degradation of rRNA by specific RNases (Deutscher 2009; Zundel et al. 2009; Basturea et al. 2011). The action of RNases on rRNA metabolism is not only ascribed to degradation pathways during low energy conditions, but also plays a major role on rRNA quality control and during the processing of pre-rRNA.

In *Escherichia coli*, rRNAs are transcribed from seven loci as preribosomal transcripts that are processed into mature rRNA forms present in ribosomes. The early processing events are carried out by RNase III (Gegenheimer et al. 1977; King and Schlessinger 1983) and correspond to endonucleolytic cleavages in two stem–loop regions encompassing 16S and 23S rRNA regions (Young and Steitz 1978; Apirion and Miczak 1993; Kaczanowska and Ryden-Aulin 2007). Kinetic analysis of newly synthesized precursors and mature rRNA indicate that RNase III processing of pre-rRNA occurs cotranscriptionally (Gegenheimer and Apirion 1975). Additional downstream cleavages by other RNases result, along with nucleotide covalent modifications, in the formation of mature 16S, 23S, and 5S fragments (Srivastava and Schlessinger 1990; Kaczanowska and Ryden-Aulin 2007). Although processing of pre-rRNA by the different nucleases can generally be carried out in the absence of previous endonucleolytic steps

[1]**Corresponding author**
E-mail malagonf@mail.nih.gov
Article published online ahead of print. Article and publication date are at http://www.rnajournal.org/cgi/doi/10.1261/rna.038588.113.

(Gegenheimer et al. 1977), proper stepwise cleavages are required for efficient downstream processing events (Li et al. 1999).

In this work, I use RNA-FISH for single cell visualization of the pre-rRNA in *E. coli*, focusing on the cellular distribution of the 5′ externally transcribed spacer (5′ETS), referred to here as the "leader," in wild type and RNase III-deficient cells. In contrast to the mature rRNA, the 5′ terminal leader region accumulates in the bacterial nucleoid area. This pattern is lost in the absence of RNase III. In addition, RNase III is required for the rapid transition from low to high rRNA synthesis occurring upon exit from stationary phase when new media is supplied for bacterial growth. Further supporting the role of RNase III on ribosomal operon induction, there is an increased requirement of the rRNA transcriptional activator Fis for cell growth in the absence of RNase III.

RESULTS AND DISCUSSION

5′ proximal pre-rRNAs preferentially localize to the nucleoid

In exponentially growing *E. coli* cells, ribosomal RNPs, visualized by following the distribution of S2 or L7/L12 ribosomal proteins, are spatially segregated from the nucleoid, suggesting that the majority of mRNA translation is in fact not directly coupled to transcription (Azam et al. 2000; Bakshi et al. 2012). The separation of nucleoid/ribosome-rich areas is further supported by the direct visualization of ribosomes in fixed cells using electron microscopy (Robinow and Kellenberger 1994). On the other hand, the distribution of pre-rRNA regions that are not incorporated into the ribosomes is not known. Gathering such information could help to understand the processing and degradation mechanisms of ribosomal operon transcripts.

In order to analyze pre-rRNA localization, I first tested and evaluated different variations of the RNA-FISH method, using the distribution of total rRNAs as a positive control. To this end, RNA-FISH analyses were done using the EUB338 probe (for simplicity referred to here as "16S probe"), which hybridizes against the highly conserved helix14 of 16S rRNA and is widely applied in bacterial taxonomy and ecology studies (Amann et al. 1990a,b; Konings and Gutell 1995). Using the protocol that gave the best signal to noise ratio (see Materials and Methods), the signal in exponentially growing *E. coli* fixed cells showed a nonhomogeneous distribution (Fig. 1A, top left). Furthermore, when compared with the nucleoid signal, obtained by DAPI staining, it became apparent that DAPI and 16S rRNAs signals do not show much overlap (Fig. 1A, top row). Microscopic analysis of cells in stationary phase showed a smaller size and a broader DAPI signal (Fig. 1A, second row). In agreement with the extensive rRNA

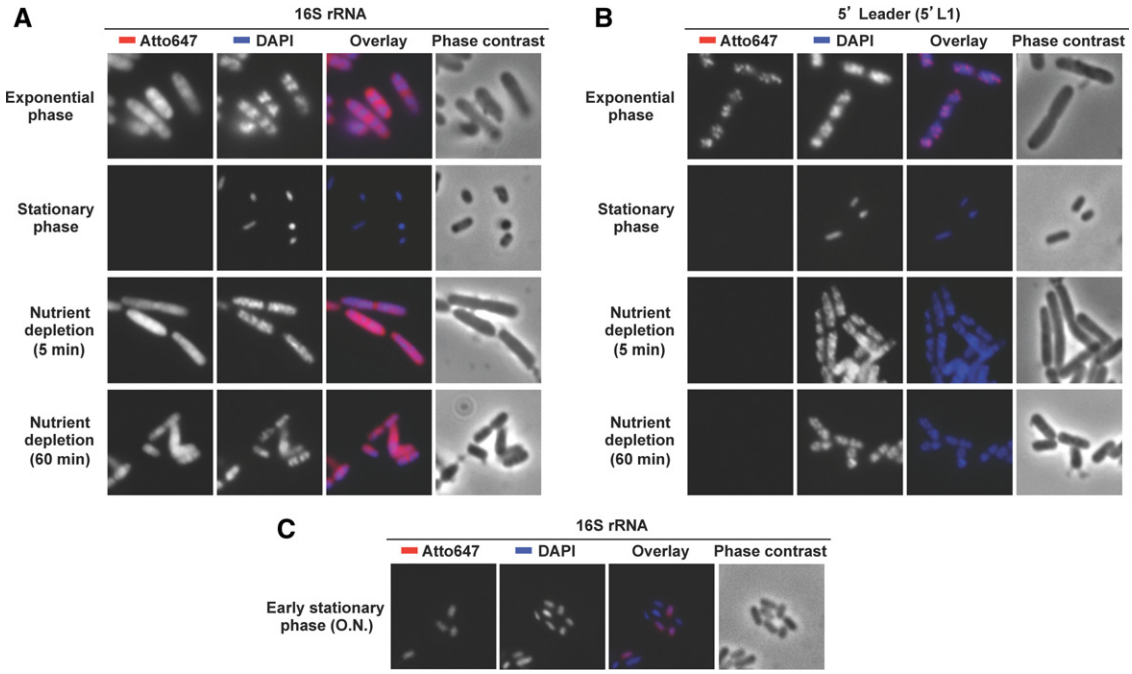

FIGURE 1. Pre-rRNA leader associates with the nucleoid. RNA-FISH analysis of wild type cells in exponential phase, stationary phase, or upon 5/60 min of nutrient deprivation, using an Atto647-labeled probes against (*A*) and (*C*) 16S rRNA, or (*B*) pre-rRNA leader (5′L1). The cells were grown in LB-Lennox for ~20 h at 37°C with shaking, and either fixed (see Materials and Methods), for stationary phase analysis, or diluted 1/200 in LB-Lennox. The freshly diluted cells were then incubated at 37°C with shaking at 225 rpm and fixed during exponential phase (after ~2 h 30 min/OD_{600} ~ 0.2), for exponential phase analysis, or spun down and incubated in carbon-source free M63 media for the indicated period of time. Atto647, DAPI, Atto647/phase contrast overlay (red/blue) and phase contrast images for each condition are shown. RNA-FISH analyses of wild type cells fixed after overnight (O.N.) growth in LB-Lennox at 37°C shown in *C*. The fake color assigned to each dye in the overlay is indicated by colored rectangles.

degradation that occurs during stationary phase (Deutscher 2003), the 16S ribosomal rRNA signal was close to or below detection level. Cells in earlier stationary phase (overnight culture), and after 1 h of nutrient deprivation, show detectable signal levels (Fig. 1C). The cellular variability in 16S signal intensity from overnight cultures is in line with the reported increase heterogeneity in cell populations during the transition from exponential to stationary phase (Makinoshima et al. 2002). Therefore, RNA-FISH analyses using fixed cells reveal a preferential localization outside of the nucleoid of 16S rRNAs, thus resembling the ribosomal cellular distribution reported previously using different techniques (Azam et al. 2000; Bakshi et al. 2012).

Due to the long half-life of ribosomal RNPs (Piir et al. 2011), probes targeting total ribosomal RNAs cannot be used reliably as tools to evaluate the transcriptional status of ribosomal operons. Conversely, pre-rRNA regions are unstable, and their levels change dramatically with environmental conditions that alter rRNA operon transcription (Cangelosi and Brabant 1997). Hence, the use of a 5′ proximal probe, targeting the RNA region located before the first described endonucleolytic cleavage site, may provide useful information about the initial site of processing/degradation of pre-rRNAs. RNA-FISH using the 5′L1 probe, complementary to the 5′ ETS from nucleotides +136 to +186, showed a preferential overlap with the cellular areas strongly stained by DAPI in exponential cells, suggesting localization to the nucleoid region (Fig. 1B, top) and no signal in cells in late stationary phase. In contrast to the 16S probe, whose signal can be readily detected in cells subject to nutrient deprivation even after 1 h, the 5′L1 probe signal is undetectable as soon as 5 min after carbon source depletion (Fig. 1, cf. A and B, third and fourth row). A corollary of this is that RNA-FISH analysis using the 5′L1 probe, alone or in combination with the 16S probe, could serve as a tool to monitor the metabolic state of single cells in heterogeneous *E. coli* populations. Interestingly, the pattern observed with the 5′L1 probe, along with the short half-life of the pre-rRNA leader, suggests that the degradation of the 5′ proximal pre-rRNA leader occurs during or shortly after the process of transcription.

RNase III cleavage is required for the preferential nucleoid localization of 5′ proximal pre-rRNA leader

RNase III is an important endonuclease (Gan et al. 2008) with a conserved protein domain present in Rnt1, Dicer, and Drosha endoribonucleases (Lamontagne et al. 2001). RNase III is the first nuclease acting on 5′ pre-rRNAs, with cleavages sites at positions +175/180 (schematized in Fig. 2A); and it is followed by the subsequent action of RNase E and RNase G (Li et al. 1999). This sequential action makes sense from the perspective of the high dependence of RNase E activity on the structure and chemical nature of RNA area upstream of the cleavage sites (Mackie 1998).

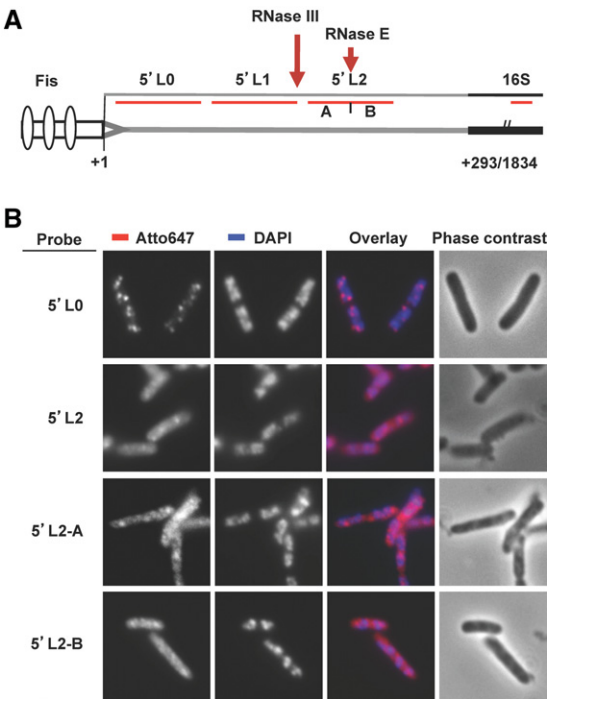

FIGURE 2. RNase III cleavage sites define the border for leader localization to the nucleoid. (*A*) Schematic representations of the ribosomal operons from P1 promoter to the 16S region indicating the coordinates for the P1 transcription start site (TSS) (+1), and for the mature 16S rRNA (+293/1834). Other features highlighted are the Fis binding sites (white ovals); the promoter (white box), leader (gray line), and 16S (black line) regions; and RNase III (+175/180) and E (+227) cleavage sites (carnelian arrows). The RNA regions hybridizing with the 5′L0, 5′L1, 5′L2, and 16S probes are marked as red lines, whereas the 5′L2-A and 5′L2-B are indicated by the letters "A" and "B" *below* the 5′L2 line. (*B*) RNA-FISH analysis of cells growing exponentially using probes hybridizing upstream of and downstream from the 5′L1 probe. Hybridization and imaging as in Figure 1.

The results obtained with probe 5′L1 showed that at least the 5′ pre-rRNA region located before the RNase III cleavage sites (5′ Proximal Pre-RRNALeader or 5P-PRL) associates with the nucleoid. This was confirmed by using the 5′L0 probe, hybridizing further upstream of the cleavage site for RNase III (Fig. 2A,B). A putative cotranscriptional processing by RNase E should also lead to enrichment in nucleoid colocalizing signal when using probes hybridizing in between the RNase III and E cleavage sites of the leader region. Nevertheless, RNA-FISH analysis using a probe (5′L2) located 3′ of the RNase III cleavage site did not revealed nucleoid enrichment (Fig. 2B). Further analysis using the probes 5′L2-A (Fig. 2A,B)—hybridizing exclusively the pre-rRNA region between the RNase III and E cleavage sites—and 5′L2-B (Fig. 2A,B)—hybridizing after the RNase E cleavage site—confirmed that the RNase III cleavage site region defines the border for nucleoid localization of 5′ pre-rRNA. This set of data suggests that RNase E processing of pre-rRNA does not occur cotranscriptionally but occurs once the partially processed pre-rRNA has left the nucleoid. This conclusion is in agreement with the reported

spatial separation of RNase E from the nucleoid (Taghbalout and Rothfield 2007; Khemici et al. 2008). Fractionation assays also indicate a possible localization of RNase III in the inner cytoplasmic membrane (Miczak et al. 1991), but this conclusion is in contradiction with the RNA-FISH results presented here and with previously reported results (Gegenheimer and Apirion 1975). Direct visualization of RNase III distribution, following an *rnc-GFP* fusion (see Materials and Methods), confirmed the lack of enrichment of RNase III in the cellular membrane area (Supplemental Fig. 1).

The RNA-FISH results using a series of probes against the 5′ leader are in agreement with a putative role for RNase III in nucleoid distribution of 5P-PRL. Consequently, the effect of deleting the *rnc* gene—encoding RNase III in *E. coli*—on pre-rRNA localization was tested. In line with the prediction, the *rnc-14* deletion allele completely disrupts the preferential nucleoid association of 5P-PRL (Fig. 3A). Thus, the localized distribution of 5P-PRL in wild type cells could be an indication of rapid processing and degradation of this fragment during or shortly after the process of transcription or, alternatively, of a role of RNase III as a quality control agent retaining pre-rRNA until properly cleaved, as shown for certain RNase protein complexes in eukaryotic systems (Hilleren et al. 2001; Jensen et al. 2001, 2003). Using a separation-of-function *rnc* mutant that retains RNA binding activity while disabling cleavage could help to discern between the two possibilities. As shown in Figure 3B, the *rnc-70* mutation, eliminating the cleavage activity of RNase III but maintaining its RNA binding activity (Li and Nicholson 1996; Dasgupta et al. 1998), did not show a strong association of pre-rRNA and DAPI signals but did show a pre-rRNA signal distribution all along the cell volume. The results presented here indicate that RNase III endonucleolytic activity governs the localization of 5P-PRL in the nucleoid and supports the proposed cotranscriptional processing of pre-rRNA by RNase III.

rnc deletion mutants are slow in rRNA operon induction and synthetically lethal with *fis*

In spite of its importance, the absence of cellular RNase III is not lethal in *E. coli* (Kindler et al. 1973; Takiff et al. 1989), a result that can be partially attributed to the existence of alternative—although inefficient without the initial action of RNase III—pre-rRNA processing pathways (Gegenheimer et al. 1977; King and Schlessinger 1983). This raises the question of why cells have evolved this complex processing mechanism for the maturation of the ribosomal operons. One possible explanation involves the use of leader sequence and its processing as a regulatory mechanism for the proper folding of rRNA (Theissen et al. 1990; Bubunenko et al. 2013). Due to the high degree of coupling shown for different steps in gene expression regulation, it is tempting to speculate that processing of the rRNA leader may play a role on coordination of other rRNA transactions.

To test a possible role of RNase III on transcription induction of ribosomal operons, RNA-FISH analyses of wild type and *rnc* mutants were repeated after 1-h outgrowth, a condition selected due to the low level of nascent pre-rRNA at time zero, the rapid induction of the ribosomal operons (Paul et al. 2004, references therein), and to the lag in cell growth in *rnc* mutants upon nutrient up-shift from stationary phase (Supplemental Fig. 2). As can be observed in Figure 4A, wild type cells showed cell morphology and rRNA signal, as evaluated with 5′L1 and 16S probes, typical of exponential growing cells after 1-h outgrowth. On the other hand, *rnc* mutants were significantly delayed on the transition to exponential metabolism using the same criteria (cf. in Fig. 4A the >95% cells with strong ribosomal signal in wild type to the ~45% in *rnc* mutants).

To further test the hypothesis of a coupling of RNase III processing with transcription activation of the ribosomal

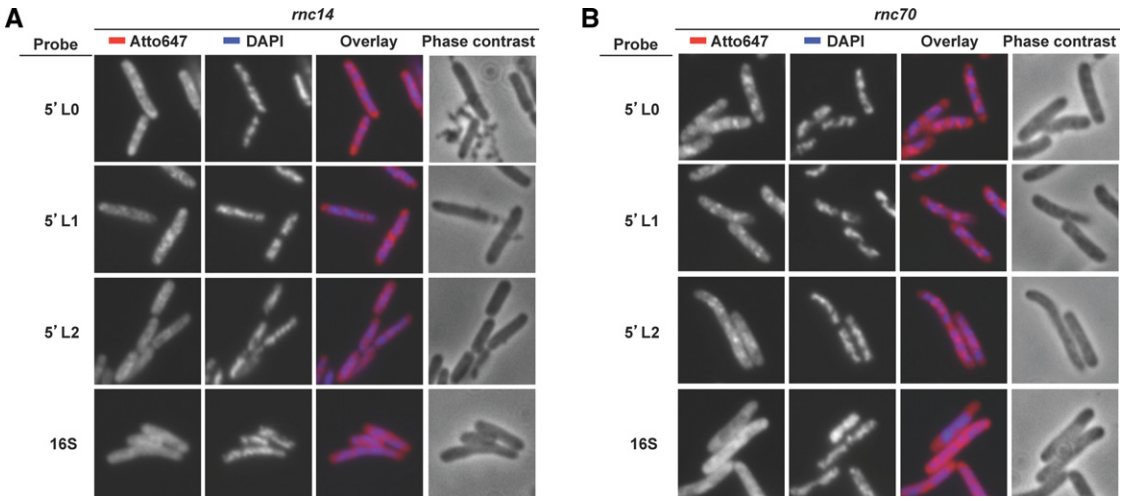

FIGURE 3. RNase III cleavage of pre-rRNA is required for nucleoid localization of 5P-PRLs. RNA-FISH analysis, using the indicated probes (see Fig. 2A), of cells growing in exponential phase containing (*A*) a nonpolar *rnc* deletion allele (*rnc14*), or (*B*) an *rnc* separation-of-function allele (*rnc70*; RNA binding^{+} RNase^{-}). Hybridization and imaging as in Figure 1.

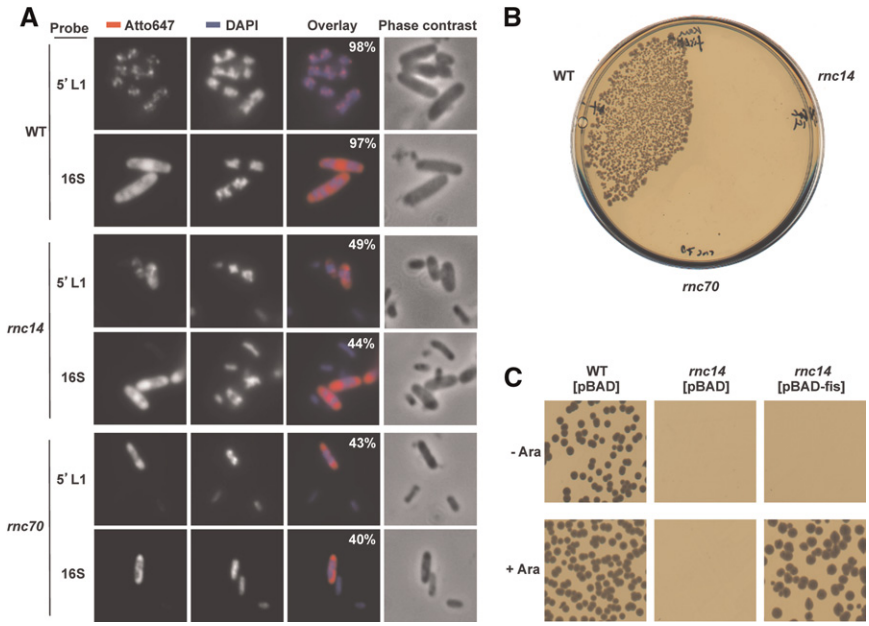

FIGURE 4. RNaseIII stimulates rapid induction of ribosomal operons and genetically interacts with Fis. (*A*) RNase III is required for optimal induction of ribosomal operons. RNA-FISH analysis of wild type (WT), *rnc14* and *rnc70* cells grown like in Figure 1 but fixed after 60 min outgrowth from stationary phase. Hybridization and imaging as in Figure 1. The percentages of cells with signal using probes 16S and 5′L1 are indicated. (*B*) P1vir phage transduction of *fisΔ::kan* deletion allele into wild type (WT), *rnc14* and *rnc70* recipient strains. The cells were plated in LB-Lennox media containing kanamycin and incubated at 37°C overnight. (*C*) P1vir phage transduction of *fisΔ::kan* deletion allele into WT and *rnc14* recipient strains transformed with an empty vector (pBAD) or the same vector containing *fis* under the control of an arabinose inducible promoter (pBAD-fis). The cells were plated in LB-Lennox media containing kanamycin with (+Ara) or without (−Ara) arabinose and incubated overnight at 37°C. Hybridization and imaging as in Figure 1.

operons, I asked if the absence of the ribosomal operon transcriptional activator Fis (Ross et al. 1990; Bokal et al. 1997; Paul et al. 2004) could exacerbate the rRNA induction defect of an *rnc* mutation. Similar to *rnc*, deletion of *fis* is not lethal (Johnson et al. 1988; Koch et al. 1988), a result attributable to the high homeostatic control of ribosomal operons (Paul et al. 2004). To obtain double *rnc fis* mutants, phage P1 generalized transduction using a Kan^R-marked deletant *fis* strain as donor, and either wild type or isogenic *rnc* deletion mutants as receptors, was performed. Although an enhanced effect on rRNA operon induction in the double mutant could have been anticipated, surprisingly the genetic interaction of *rnc* and *fis* was stronger than expected since no viable double mutants could be obtained (Fig. 4B). A possible defect of *rnc* strains as receptor in phage P1 transduction was ruled out by repeating the transduction of the *fisΔ::kan* allele to an *rnc* recipient strain containing a plasmid expressing *fis* only when arabinose was added to the media (Fig. 4C). The interplay of *fis* and *rnc* mutations indicates an essential requirement of Fis for cell viability in the absence of RNase III and suggests that Fis-mediated transcription activation is critical for ribosomal operon transcription in the absence of RNase III.

A role for RNase III influence on ribosomal operon transcription?

The data presented here may indicate an effect on RNase III on ribosome operon transcription. In spite of the novelty of this concept, previous research data fit this idea. The cotranscriptional coupling of RNase III processing has already been established (Gegenheimer and Apirion 1975) and is further supported by this work. Interestingly, classic electron microscopy analysis of wild type and *rnc* mutants should be re-evaluated in light of a recent paper describing a correlation between RNA polymerase distribution and speed on the ribosomal operons (Dennis et al. 2009). The nascent pre-rRNPs grow steadily as the polymerases transcribe 5′ to 3′ from the leader to the spacer region (between 16S and 23S regions) and is followed by a re-establishment of the gradient in the spacer (Quan et al. 2005). Concomitantly, there is a decrease in the number of transcription complexes per nucleotide in the leader and spacer (Quan et al. 2005), a result that suggests an increased speed of the RNA polymerase in these areas (Dennis et al. 2009). In the absence of RNase III, not only the double pre-rRNP length gradient is lost but also the relative RNA polymerase occupancy in the spacer and nonspacer regions are approximately similar (Hofmann and Miller 1977; French and Miller 1989).

I propose, as a working model, that the nascent pre-16S rRNPs, and by extension pre-23S rRNPs, need to be uncoupled from the elongating RNA polymerases by RNase III for efficient transcription. In this model, that I nicknamed the "Atlas model" due to the postulation that nascent pre-rRNP may represent a heavy burden for RNA polymerase transcription, cotranscriptional pre-rRNA cleavage by RNase III relieves the transcription apparatus of the heavily decorated pre-rRNA still attached to the polymerase after synthesis of the 16S copy (Supplemental Fig. 3). Moreover, cotranscriptional release of pre-16S rRNP, and again pre-23S rRNP, would facilitate the rapid segregation of ribosomal particles to the space outside of the nucleoid (Bakshi et al. 2012). Upon cleavage by RNase III, 5P-PRL remains in the nucleoid, where it is degraded, and the pre-16S rRNP is translocated to the "cytoplasmic region." Not only the aforementioned electron microscopy analysis fits the model but also RNA localization analysis of the ITS between the 16 and 23 S loops, using a probe hybridizing against nucleotides +2206 to +2255 (immediately upstream of the RNase III cleavage site on the 23S loop) (Supplemental Fig. 4).

An important follow-up point is how the DAPI-enriched pre-rRNA fragments are confined to the nucleoid area. One possibility is that the nucleoid-associated pre-rRNA fragments do indeed diffuse to the ribosome rich areas but are rapidly degraded by RNases, thus preventing their detection. I disfavor this possibility on account of the strong signal observed outside the DAPI region when using probes targeting pre-rRNA leader regions located immediately downstream from the RNase III cleavage site (Fig. 2B). Additionally, since *E. coli* does not have 5′-3′ RNases, it would be expected to detect signal all over the cells when using the 5′ end-proximal probe (5′L0), even more so when taking into account the high level of RNA secondary structure right upstream of the RNase III cleavage site. An alternative explanation is the existence of a specific nucleoid retention factor for some pre-rRNA fragments. Although RNase III could theoretically be that factor, this protein does not have a localized cellular distribution (Supplemental Fig. 1), nor is the separation of function *rnc70* allele able to provide nucleoid retention capabilities. Recently, Bubunenko et al. (2013) have shown a striking interplay between the Nus factors and RNase III on the modulation of pre-rRNA biogenesis. Nus proteins bind both the pre-rRNA boxA loop, located upstream of the RNase III cleavage sites on the leader and internal spacer, and RNA polymerase. Altogether, this makes the Nus complex an optimal candidate for a factor mediating the regulation of pre-rRNA localization.

MATERIALS AND METHODS

Bacterial strains and plasmids

Wild type K-12 *E. coli* strain MG1655 (F- λ- *ilvG- rfb*-50 *rph*-1) has been previously described (Blattner et al. 1997). The mutant strains used are isogenic to MG1655 and were constructed by introducing into the wild type the *rnc-14Δ::Tn10*^{tetR} (Takiff et al. 1989), *rnc70 TD1-17Δ::Tn10*^{tetR} (Dasgupta et al. 1998), and *fisΔ::Kan*^{R} (Baba et al. 2006) alleles by P1kc transduction (Lennox 1955). The plasmid pBAD24 is an Amp^{R} multicopy expression plasmid containing the *araBAD* promoter (Guzman et al. 1995). Plasmid pBAD24-fis was constructed by placing the *fis* ORF under the control of the *araBAD* promoter. To this end, an *Eco*RI/*Sma*I PCR fragment was obtained using genomic DNA of MG1655 as template and the oligos fis-ecori-5′ (CCGCGAATTCGCCAATGTTCGAACAACGCGTAAATTCT).

fis-smaI-3′ (ATTATCCCGGGTCACTCCCTTTGTGACACCTA TAA) was cloned into pBAD24 opened with *Eco*RI and *Sma*I. The plasmid pBAD24-rnc-sfGFP (GenBank ID: KF020495), contains the *rnc* gene fused to the N terminus of a superfolder enhanced GFP gene. The sfGFP fragment was created using gene synthesis technology (Excellgen), taking as template a superfolder enhanced GFP gene sequence optimized for *E. coli* expression (GenBank ID: HQ873313.1), and cloned into pBAD24 using the oligos sfGFP-Eco-linker-5′ (CCGCGAATTCGCCAATGGCTCGAGCCCGGGC GCGTAAAGGCGAAGAG) and sfGFP-XbaI-linker-3′ (CCTCCT CCAATCTAGACCTTTGTACAGTTCATCCATACCATG) to create the plasmid pBAD24-sfGFPx2 (GenBank ID: KF020494). The *rnc* ORF was amplified from genomic DNA using the oligos rnc-ecori-5′ (CCGCGAATTCGCCAATGAACCCCATCGTAA) rnc-xhoI-3′ (TTTATCTCGAGGTTCCAGCTCCAGTTTTTTC), and cloned into *Eco*RI-*Xho*I of pBAD24-sfGFPx2. Positive clones were scored by restriction mapping and by visualization of green fluorescence of colonies grown in arabinose containing media using a Dark Reader blue light transilluminator with an amber screen (Clare-chemical).

Cell growth conditions, fixation procedure, probes, and probe labeling

Cells were grown at 37°C in LB-Lennox media with shaking at 225 rpm unless indicated otherwise. For nutrient depletion experiments, bacteria growing exponentially in LB-Lennox were spun down for 1 min and incubated in carbon-source free M63 minimal medium at 37°C with shaking for either 5 or 60 min before fixation. In experiments requiring expression from pBAD24 plasmids, arabinose was added to a final 0.1% concentration. The cultures were fixed, adding formaldehyde to a final concentration of 4% and incubating the cells for 1 h. Fixed cells were washed three times with PBS and kept at 4°C. Probe 16S (GCTGCC**T**CCCGTAGGAGT) has been described previously with the name EUB338 (Amann et al. 1990a). As probes specific for the pre-rRNA leader, I used the *rrnB* oligonucleotides 5′L0 (ATACGCC**T**TCCCGCTACAGAG**T**CAAGCATTTA **T**TTTTGCTTTC**T**CTGCCG), 5′L1 (TGCCCACACAGA**T**TGTCT GATAAATTG**T**TAAAGAGCAGTGCCGC**T**TCGCT), 5′L2 (TGTT CACTCT**T**GAGACTTGGTAT**T**CATTTTTCGTCT**T**GCGACGTT AAGAAT), 5′L2-A (TCATT**T**TTCGTCTTGCGACG**T**TAAGAAT), and 5′L2-B (TGT**T**CACTCTTGAGACT**T**GGTAT). Probe ITS1 (CTTTCGA**T**TCATCATCGTG**T**TGCGAAAA**T**TTGAGAGAC**T**CA CGAACAACT) hybridizes against the spacer pre-rRNA region located immediately upstream of the pre-23S loop RNase III cleavage site. In all the probes, the T nucleotides in bold represent an amino modified C6 dT, suitable for fluorophore conjugation (IDT technologies). The probes were labeled with Atto647N NHS ester (Fluka).

RNA-FISH

Bacterial RNA-FISH procedure was done by modifying a yeast-optimized protocol (Malagon and Jensen 2008). Briefly, fixed cells were washed with PBS, subjected to an enzymatic treatment with lysozyme to eliminate the bacterial cell wall (10 mg/mL lysozyme >40,000 units/mg of protein, in PBS containing 0.1 volume of ribonucleoside vanadyl complex, 45 min at 30°C), followed by membrane permeabilization with cold ethanol 70%. After two washes with PBS, cells were preincubated with hybridization solution for 30 min, followed by an overnight incubation at 37°C with the fluorescent probe. Two times SSC, 40% formamide, 12% dextran sulfate (average MW >500,000, Sigma-Aldrich), 1% ribonucleoside vanadyl complex, salmon sperm DNA 0.1 mg/mL; yeast tRNA 0.1 mg/mL, BSA 0.1 mg/mL, and heat denatured probe at 500 ng/mL was used as hybridization solution. After incubation, cells were washed for 30 min four times, twice at 37°C and twice at room temperature, in prehybridization solution, followed by a 5-min wash with PBS. Cells were added to coverslips pretreated with polylysine, incubated at room temperature for 1 h, mounted with DAPI-containing vectashield mounting solution (Vector Laboratories), and visualized after placed and sealed on microscopy slides.

Imaging

Imaging was done using an Eclipse E100 epifluorescence microscope (Nikon) equipped with a SensiCam-qe camera (Cooke), a Light Engine S/N 1240 illumination source (Lumecor), and a FF410/504/582/669-Di01-25 × 26-QF multiwavelengh filter (Semrock). The slides were visualized using a 100× CFI Plan Apo Ph3 DM objective (Nikon) and 1.5 refraction index Type DF immersion oil (Cargille Laboratories). DAPI, GFP, and fluorescence-labeled probes were visualized after illumination with beams of 390 ± 9, 485 ± 20, and 650 ± 7 nm, respectively. All probe images were taken with binning 1 and using near similar exposure times and image scaling when using the same probe. All panels in the figures have an original lateral size of 150 pixels (9.675 µm). We used Metamorph 7.6.4.0 software (Molecular Devices) for image acquisition and Adobe Photoshop for image handling.

SUPPLEMENTAL MATERIAL

Supplemental material is available for this article.

ACKNOWLEDGMENTS

I thank Sankar Adhya for his constant and generous scientific and financial support and for critical comments on this manuscript. I also thank Donald Court, Susan Gottesman, and Nadim Majdalani for strains and plasmids; Donald Court, Brian Peddie, and Nadim Majdalani for comments; and Cindy Clark, NIH Library Writing Center, for manuscript editing assistance. This research was supported by the Intramural Research Program of the National Institutes of Health, National Cancer Institute, Center for Cancer Research.

Received February 7, 2013; accepted June 14, 2013.

REFERENCES

Amann RI, Binder BJ, Olson RJ, Chisholm SW, Devereux R, Stahl DA. 1990a. Combination of 16S rRNA-targeted oligonucleotide probes with flow cytometry for analyzing mixed microbial populations. *Appl Environ Microbiol* **56:** 1919–1925.

Amann RI, Krumholz L, Stahl DA. 1990b. Fluorescent-oligonucleotide probing of whole cells for determinative, phylogenetic, and environmental studies in microbiology. *J Bacteriol* **172:** 762–770.

Apirion D, Miczak A. 1993. RNA processing in prokaryotic cells. *Bioessays* **15:** 113–120.

Azam TA, Hiraga S, Ishihama A. 2000. Two types of localization of the DNA-binding proteins within the *Escherichia coli* nucleoid. *Genes Cells* **5:** 613–626.

Baba T, Ara T, Hasegawa M, Takai Y, Okumura Y, Baba M, Datsenko KA, Tomita M, Wanner BL, Mori H. 2006. Construction of *Escherichia coli* K-12 in-frame, single-gene knockout mutants: The Keio collection. *Mol Syst Biol* **2:** 2006.0008.

Bakshi S, Siryaporn A, Goulian M, Weisshaar JC. 2012. Superresolution imaging of ribosomes and RNA polymerase in live *Escherichia coli* cells. *Mol Microbiol* **85:** 21–38.

Basturea GN, Zundel MA, Deutscher MP. 2011. Degradation of ribosomal RNA during starvation: Comparison to quality control during steady-state growth and a role for RNase PH. *RNA* **17:** 338–345.

Blattner FR, Plunkett G III, Bloch CA, Perna NT, Burland V, Riley M, Collado-Vides J, Glasner JD, Rode CK, Mayhew GF, et al. 1997. The complete genome sequence of *Escherichia coli* K-12. *Science* **277:** 1453–1462.

Bokal AJ, Ross W, Gaal T, Johnson RC, Gourse RL. 1997. Molecular anatomy of a transcription activation patch: FIS-RNA polymerase interactions at the *Escherichia coli rrnB* P1 promoter. *EMBO J* **16:** 154–162.

Bubunenko M, Court DL, Al Refaii A, Saxena S, Korepanov A, Friedman DI, Gottesman ME, Alix JH. 2013. Nus transcription elongation factors and RNase III modulate small ribosome subunit biogenesis in *Escherichia coli*. *Mol Microbiol* **87:** 382–393.

Cangelosi GA, Brabant WH. 1997. Depletion of pre-16S rRNA in starved *Escherichia coli* cells. *J Bacteriol* **179:** 4457–4463.

Dahan N, Choder M. 2013. The eukaryotic transcriptional machinery regulates mRNA translation and decay in the cytoplasm. *Biochim Biophys Acta* **1829:** 169–173.

Dasgupta S, Fernandez L, Kameyama L, Inada T, Nakamura Y, Pappas A, Court DL. 1998. Genetic uncoupling of the dsRNA-binding and RNA cleavage activities of the *Escherichia coli* endoribonuclease RNase III—the effect of dsRNA binding on gene expression. *Mol Microbiol* **28:** 629–640.

Dennis PP, Ehrenberg M, Fange D, Bremer H. 2009. Varying rate of RNA chain elongation during *rrn* transcription in *Escherichia coli*. *J Bacteriol* **191:** 3740–3746.

Deutscher MP. 2003. Degradation of stable RNA in bacteria. *J Biol Chem* **278:** 45041–45044.

Deutscher MP. 2009. Maturation and degradation of ribosomal RNA in bacteria. *Prog Mol Biol Transl Sci* **85:** 369–391.

French SL, Miller OL Jr. 1989. Transcription mapping of the *Escherichia coli* chromosome by electron microscopy. *J Bacteriol* **171:** 4207–4216.

Gan J, Shaw G, Tropea JE, Waugh DS, Court DL, Ji X. 2008. A stepwise model for double-stranded RNA processing by ribonuclease III. *Mol Microbiol* **67:** 143–154.

Gegenheimer P, Apirion D. 1975. *Escherichia coli* ribosomal ribonucleic acids are not cut from an intact precursor molecule. *J Biol Chem* **250:** 2407–2409.

Gegenheimer P, Watson N, Apirion D. 1977. Multiple pathways for primary processing of ribosomal RNA in *Escherichia coli*. *J Biol Chem* **252:** 3064–3073.

Guzman LM, Belin D, Carson MJ, Beckwith J. 1995. Tight regulation, modulation, and high-level expression by vectors containing the arabinose P_{BAD} promoter. *J Bacteriol* **177:** 4121–4130.

Hilleren P, McCarthy T, Rosbash M, Parker R, Jensen TH. 2001. Quality control of mRNA 3′-end processing is linked to the nuclear exosome. *Nature* **413:** 538–542.

Hofmann S, Miller OL Jr. 1977. Visualization of ribosomal ribonucleic acid synthesis in a ribonuclease III-deficient strain of *Escherichia coli*. *J Bacteriol* **132:** 718–722.

Jensen TH, Patricio K, McCarthy T, Rosbash M. 2001. A block to mRNA nuclear export in *S. cerevisiae* leads to hyperadenylation of transcripts that accumulate at the site of transcription. *Mol Cell* **7:** 887–898.

Jensen TH, Dower K, Libri D, Rosbash M. 2003. Early formation of mRNP: License for export or quality control? *Mol Cell* **11:** 1129–1138.

Johnson RC, Ball CA, Pfeffer D, Simon MI. 1988. Isolation of the gene encoding the Hin recombinational enhancer binding protein. *Proc Natl Acad Sci* **85:** 3484–3488.

Kaczanowska M, Ryden-Aulin M. 2007. Ribosome biogenesis and the translation process in *Escherichia coli*. *Microbiol Mol Biol Rev* **71:** 477–494.

Khemici V, Poljak L, Luisi BF, Carpousis AJ. 2008. The RNase E of *Escherichia coli* is a membrane-binding protein. *Mol Microbiol* **70:** 799–813.

Kindler P, Keil TU, Hofschneider PH. 1973. Isolation and characterization of a ribonuclease 3 deficient mutant of *Escherichia coli*. *Mol Gen Genet* **126:** 53–59.

King TC, Schlessinger D. 1983. S1 nuclease mapping analysis of ribosomal RNA processing in wild type and processing deficient *Escherichia coli*. *J Biol Chem* **258:** 12034–12042.

Koch C, Vandekerckhove J, Kahmann R. 1988. *Escherichia coli* host factor for site-specific DNA inversion: Cloning and characterization of the *fis* gene. *Proc Natl Acad Sci* **85:** 4237–4241.

Konings DA, Gutell RR. 1995. A comparison of thermodynamic foldings with comparatively derived structures of 16S and 16S-like rRNAs. *RNA* **1:** 559–574.

Lamontagne B, Larose S, Boulanger J, Elela SA. 2001. The RNase III family: A conserved structure and expanding functions in eukaryotic dsRNA metabolism. *Curr Issues Mol Biol* **3:** 71–78.

Lennox ES. 1955. Transduction of linked genetic characters of the host by bacteriophage P1. *Virology* **1:** 190–206.

Li H, Nicholson AW. 1996. Defining the enzyme binding domain of a ribonuclease III processing signal. Ethylation interference and hydroxyl radical footprinting using catalytically inactive RNase III mutants. *EMBO J* **15:** 1421–1433.

Li Z, Pandit S, Deutscher MP. 1999. RNase G (CafA protein) and RNase E are both required for the 5′ maturation of 16S ribosomal RNA. *EMBO J* **18:** 2878–2885.

Luna R, Gaillard H, González-Aguilera C, Aguilera A. 2008. Biogenesis of mRNPs: Integrating different processes in the eukaryotic nucleus. *Chromosoma* **117:** 319–331.

Mackie GA. 1998. Ribonuclease E is a 5′-end-dependent endonuclease. *Nature* **395:** 720–723.

Makinoshima H, Nishimura A, Ishihama A. 2002. Fractionation of *Escherichia coli* cell populations at different stages during growth transition to stationary phase. *Mol Microbiol* **43:** 269–279.

Malagon F, Jensen TH. 2008. The T body, a new cytoplasmic RNA granule in *Saccharomyces cerevisiae*. *Mol Cell Biol* **28:** 6022–6032.

Maniatis T, Reed R. 2002. An extensive network of coupling among gene expression machines. *Nature* **416:** 499–506.

Miczak A, Srivastava RA, Apirion D. 1991. Location of the RNA-processing enzymes RNase III, RNase E and RNase P in the *Escherichia coli* cell. *Mol Microbiol* **5:** 1801–1810.

Miller OL Jr, Hamkalo BA, Thomas CA Jr. 1970. Visualization of bacterial genes in action. *Science* **169:** 392–395.

Muhlemann O, Jensen TH. 2012. mRNP quality control goes regulatory. *Trends Genet* **28:** 70–77.

Paul BJ, Ross W, Gaal T, Gourse RL. 2004. rRNA transcription in *Escherichia coli*. *Annu Rev Genet* **38:** 749–770.

Piir K, Paier A, Liiv A, Tenson T, Maivali U. 2011. Ribosome degradation in growing bacteria. *EMBO Rep* **12:** 458–462.

Quan S, Zhang N, French S, Squires CL. 2005. Transcriptional polarity in rRNA operons of *Escherichia coli nusA* and *nusB* mutant strains. *J Bacteriol* **187:** 1632–1638.

Robinow C, Kellenberger E. 1994. The bacterial nucleoid revisited. *Microbiol Rev* **58:** 211–232.

Ross W, Thompson JF, Newlands JT, Gourse RL. 1990. *E.coli* Fis protein activates ribosomal RNA transcription *in vitro* and *in vivo*. *EMBO J* **9:** 3733–3742.

Schneider DA, Gaal T, Gourse RL. 2002. NTP-sensing by rRNA promoters in *Escherichia coli* is direct. *Proc Natl Acad Sci* **99:** 8602–8607.

Srivastava AK, Schlessinger D. 1990. Mechanism and regulation of bacterial ribosomal RNA processing. *Annu Rev Microbiol* **44:** 105–129.

Taghbalout A, Rothfield L. 2007. RNaseE and the other constituents of the RNA degradosome are components of the bacterial cytoskeleton. *Proc Natl Acad Sci* **104:** 1667–1672.

Takiff HE, Chen SM, Court DL. 1989. Genetic analysis of the *rnc* operon of *Escherichia coli*. *J Bacteriol* **171:** 2581–2590.

Theissen G, Behrens SE, Wagner R. 1990. Functional importance of the *Escherichia coli* ribosomal RNA leader box A sequence for post-transcriptional events. *Mol Microbiol* **4:** 1667–1678.

Young RA, Steitz JA. 1978. Complementary sequences 1700 nucleotides apart form a ribonuclease III cleavage site in *Escherichia coli* ribosomal precursor RNA. *Proc Natl Acad Sci* **75:** 3593–3597.

Zundel MA, Basturea GN, Deutscher MP. 2009. Initiation of ribosome degradation during starvation in *Escherichia coli*. *RNA* **15:** 977–983.